Organic & Biomolecular Chemistry

Chromic Properties of Dibenzo[j,l]fluoranthenes Exhibiting Different Resonance Contribution

Journal:	*Organic & Biomolecular Chemistry*
Manuscript ID	OB-ART-05-2024-000750.R1
Article Type:	Paper
Date Submitted by the Author:	23-May-2024

Complete List of Authors:	Kurokawa, Kazuma; Kyoto University, Graduate School of Pharmaceutical Sciences Ogawa, Naoki; Kyoto University, Graduate School of Pharmaceutical Sciences Kuroda, Yusuke; Kyoto University, Graduate School of Pharmaceutical Sciences Yamaoka, Yousuke; Kyoto University, Graduate School of Pharmaceutical Sciences Takikawa, Hiroshi; Kyoto University, Graduate School of Pharmaceutical Sciences Tsubaki, Kazunori; Kyoto Prefectural University, Graduate School of Life and Environmental Sciences Takasu, Kiyosei; Kyoto University, Graduate School of Pharmaceutical Sciences

ARTICLE

Chromic Properties of Dibenzo[*j,l*]fluoranthenes Exhibiting Different Resonance Contribution

Received 00th January 20xx,
Accepted 00th January 20xx

DOI: 10.1039/x0xx00000x

Kazuma Kurokawa,[a] Naoki Ogawa,[a] Yusuke Kuroda,[a] Yousuke Yamaoka,[a] Hiroshi Takikawa,[a] Kazunori Tsubaki[b] and Kiyosei Takasu*[a]

Chromic molecules change colour in response to external stimuli and are utilized in applications such as food additive detection, light dimmers, and biological probes. One of the common design strategies of organic chromic molecules is based on changes in the π-conjugation. We have hypothesized that non-alternant polyaromatic hydrocarbon (PAH) skeletons can be used as a backbone for chromic molecules. Herein, we synthesized hydroxy-substituted dibenzo[*j,l*]fluoranthenes, a class of non-alternant PAHs, as novel chromic compounds and evaluated their halochromic properties by UV-vis and fluorescence spectroscopy. Under basic conditions, the 1-hydroxy derivatives show hyperchromic shift, whereas the 9-hydroxy derivatives show bathochromic shift and fluorescence although the skeleton of chromophore is same. Density functional theory calculations indicated that the different chromic properties are attributed to the difference in their resonance structures.

1. Introduction

Chromism is the reversible colour change that a compound undergoes induced by external stimuli (pH, solvent, heat, light, mechanical stimuli, etc.) and is used for food additive detection,[1] light dimmers,[2] and biological probes.[3] The design strategies of organic chromic molecules are usually based on changes in the π-conjugation[3a,4] or molecular aggregation of long linearly conjugated molecules.[5] Polycyclic aromatic hydrocarbons (PAHs) have also attracted considerable attention as chromophores because of their expected absorption in the visible and near-infrared regions.[6] Fluoranthenes, whose skeleton contains benzene and naphthalene units connected by a pentagonal carbocycle, represent a class of non-alternant PAHs. Fluoranthenes are found not only in incomplete combustion products as pollutants,[7] but also in nature as biologically active compounds.[8] The fluoranthene core is also utilised as a chromophore in materials science. Fluoranthene derivatives have been developed for use in fluorescent sensors,[9] optoelectronic devices,[10] and dye-sensitised solar cells.[11]

Several efforts for the syntheses of fluoranthene derivatives have been reported,[12] and recently we have also achieved the synthesis of π-extended fluoranthenes by a domino reaction (Scheme 1).[13] Thus, a reaction of biaryl compound **1a** bearing

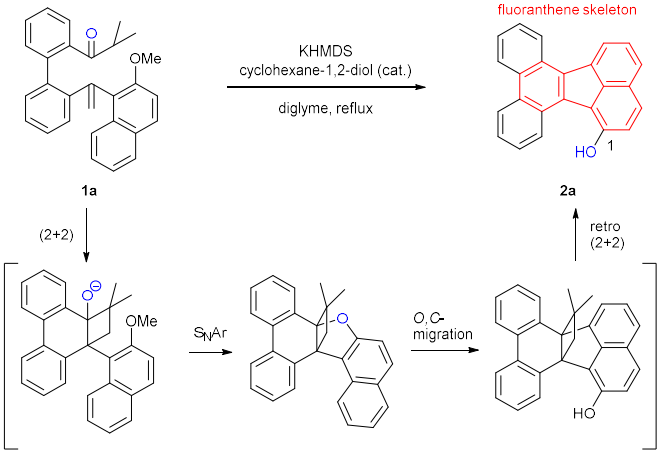

Scheme 1 A domino reaction giving dibenzofluoranthene **2a.**

acyl and naphthylalkenyl moieties with KHMDS afforded 1-hydroxydibenzo[*j,l*]fluoranthenes **2a** via (2+2) cycloaddition–S_NAr–*O,C* migration–retro (2+2) cycloaddition sequence.

During the course of our study, we found that the UV-vis absorbance of **2a** changed reversibly depending on the pH of the solution (halochromism). The chromic property of **2a** was analysed by UV-vis and fluorescence spectroscopy under neutral and basic conditions in CH_2Cl_2 solution (Fig. 1). The absorption spectrum of **2a** exhibited major bands at 400 nm (moderate) and 420–500 nm (broad, weak) under neutral conditions (Fig. 1a, black line). When 1,8-diazabicyclo[5.4.0]undec-7-ene (DBU) was added to **2a**, the absorption at 450 nm gradually increased and became saturated with the addition of 1.0 equivalent of DBU (Fig. 1a,

[a] *Graduate School of Pharmaceutical Sciences, Kyoto University, Yoshida, Sakyo-ku, Kyoto 606-8501, Japan.*
[b] *Graduate School of Life and Environmental Sciences, Kyoto Prefectural University, Shimogamo, Sakyo-ku, Kyoto 606-8522, Japan.*
Electronic Supplementary Information (ESI) available: [details of any supplementary information available should be included here]. See DOI: 10.1039/x0xx00000x

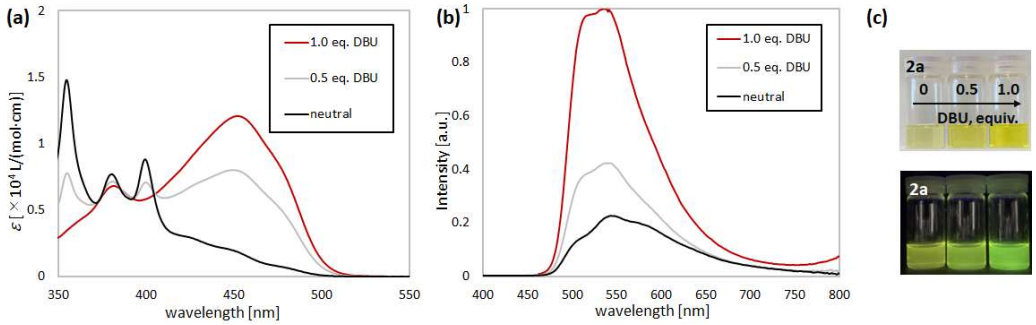

Fig. 1 (a) UV-vis absorption and (b) fluorescence spectra of **2a** in CH_2Cl_2, added with DBU at 296 K (λ_{ex} = 381 nm). (c) The colour change of **2a** under daylight (above) and 365nm-UV irradiation (bottom) with addition of DBU.

red line, basic conditions). In contrast, the absorption spectrum was not changed although excess amount of trifluoroacetic acid (TFA) was added (acidic conditions, see SI; Fig. S3). The emission spectrum of **2a** shows yellow-green fluorescence at 543 nm (λ_{ex} = 381 nm) under neutral conditions (Fig. 1b, black line). When DBU was added to the solution of **2a**, the fluorescence was dramatically strengthened at almost the same wavelength (Fig. 1b, red line). For **2a**, the obtained fluorescence quantum yield was 3.9% under neutral conditions, and it increased to 8.7% when DBU was added (see, Table 1). Reversible photophysical changes in **2a** with DBU were observed upon the addition of TFA. The colour change is accompanied by isosbestic points. This means that the resonance system of the dibenzofluoranthene skeleton, which is composed of naphthalene and phenanthrene rings, is largely recombined by the change in pH.

We envisaged that the introduction of an auxochrome, such as a hydroxy group, at the appropriate position in the chromophore would induce characteristic chromic properties depending on the resulting resonance hybrid. We designed two types of hydroxy-substituted dibenzo[*j,l*]fluoranthenes, with substitutions at positions 1 and 9, viz. **2** and **3**, respectively. We expected that the resonance contribution could be controlled by adjusting the position of the hydroxy substituent. Thus, the contribution of the fluorenyl-type structure increased in the anion of **2**, whereas that of the quinoid-type resonance increased in the anion of **3** (Fig. 2). Herein, we report the syntheses and photophysical properties of

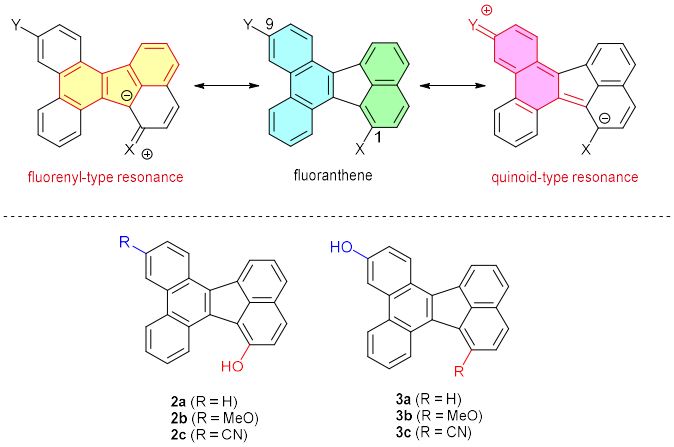

Fig. 2 Typical resonance structures of dibenzofluoranthene and designed dibenzo[*j,l*]fluoranthenes **2a–c** and **3a–c**.

dibenzo[*j,l*]fluoranthenes bearing a hydroxy group, which exhibit halochromism in their UV-vis absorption and fluorescence spectra based on changes in their π-conjugation states.

2. Results and Discussion

2.1 Synthesis of hydroxydibenzofluoranthenes.

We designed 1-hydroxy-9-methoxydibenzo[*j,l*]fluoranthene (**2b**) as a common synthetic intermediate for the synthesis of **2c** and **3a–c** (Scheme 2). In line with our previous report,[13] the treatment of biaryl ketone **1b** with KHMDS afforded 1-hydroxy-9-methoxy derivative **2b** in 62% yield. Subsequent triflation of **2b** produced compound **5** in 86% yield, which, upon Pd-catalysed reduction in the presence of Et_3SiH and followed by demethylation using BBr_3, led to the formation of 9-hydroxyfluoranthene **3a** in 70% yield (two steps). Pd-catalysed cyanation of **5**, followed by demethylation using a thiolate anion, afforded 1-cyano-9-hydroxy derivative **3c** in 62% yield (two steps). 9-Hydroxy-1-methoxy **3b** was synthesized from **2b** in three steps. Thus, methylation of **2b** gave 1,9-dimethoxy derivative **6** in 91% yield. When **6** was treated with a slightly excess amount of BBr_3 (1.34 equiv) at 20 °C, demethylation at the less hindered methyl ether mainly proceeded to give 9-hydroxy-1-methoxy **3b** in 51% yield. 9-Cyano-1-hydroxy derivative **2c** was also prepared from **3b**, following the synthetic route of **3c** from **2b**. The control compound, non-hydroxy derivative **4**, was synthesized from **2a** in 98% yield.

Single crystals of **2b** suitable for X-ray crystallographic analysis were successfully grown by slow diffusion of hexane into the solution of **2b** in ethyl acetate (Fig. 3). Its dibenzofluoranthane skeleton of **2b** is completely planar.

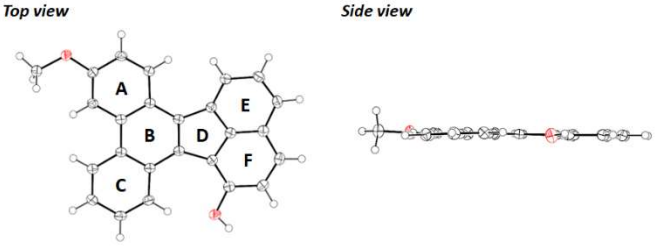

Fig. 3 X-ray crystallographic structure of **2b** (CCDC2251568).

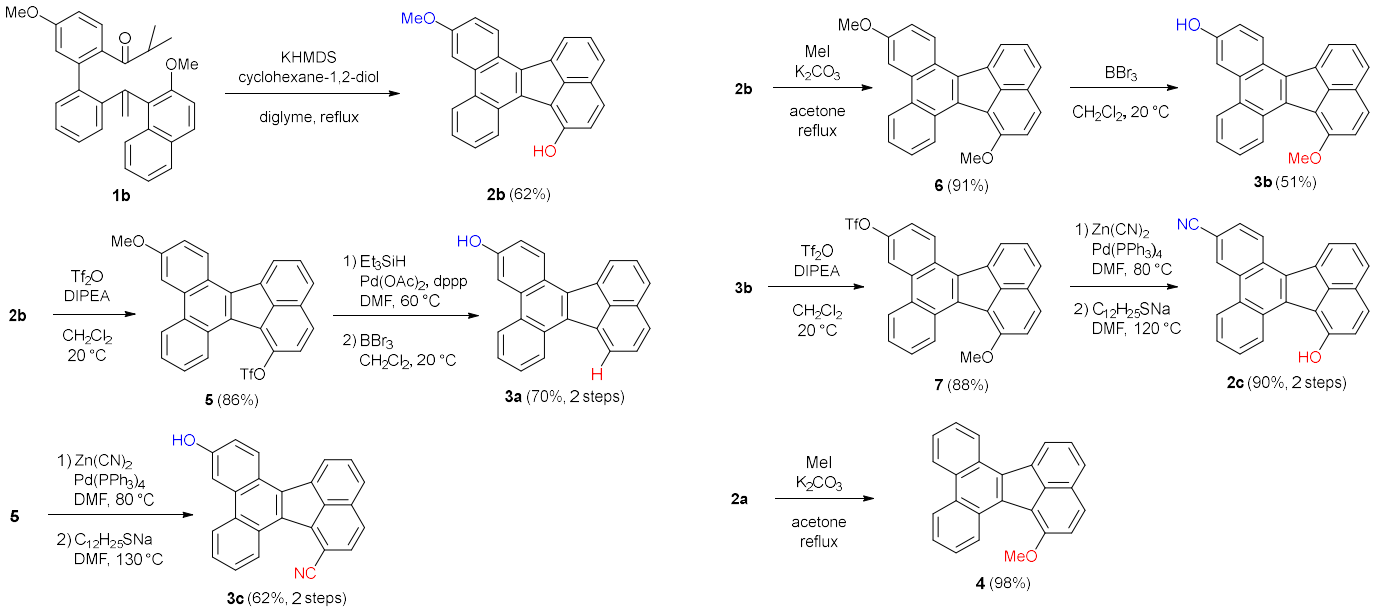

Scheme 2 Preparation of **2b–c**, **3a–c** and **4**.

2.2 Photophysical characterization of 2 and 3.

Initially, to validate our working hypothesis, the photophysical properties of non-hydroxy derivative **4** were investigated (Fig. 4a). Unlike compound **2a**, almost identical UV-vis absorption spectra were observed for **4** in the absence or presence of DBU. This observation strongly suggests that the chromic behaviour of **2a** is induced by the deprotonation of its phenolic proton. Next, we explored the substitution effect at the 9 position of 1-hydroxyfluoranthene **2**. The series of **2** exhibited similar absorption and emission spectra and hyperchromic properties, regardless of whether the substituent was electron-donating (**2b**) or electron-withdrawing (**2c**) groups (Fig. 4b–f). The fluorescence quantum yields (Φ) of **2** in CH_2Cl_2 were weak (Table 1). Notably, Φ values of **2** under basic conditions (in the presence of DBU) were higher than those under neutral conditions, with **2c** showing the highest quantum yield (10%) under basic conditions. The fluorescence lifetimes (τ) of **2** under neutral and basic conditions were determined using time-correlated single photon counting method in CH_2Cl_2. As the result, it was found that the radiative rate constants ($k_F = \Phi/\tau$) of **2a** increased with the addition of DBU (1.29×10^7 s^{-1} under neutral conditions; 3.11×10^7 s^{-1} under basic conditions).

Interestingly, the chromic properties of 9-hydroxy derivatives **3** differed from those of 1-hydroxy derivatives **2** (Fig. 5 and Table 2). Under neutral conditions, **3a** exhibited major bands at 400 nm (moderate) and 410–530 nm (broad, weak). However, upon addition of DBU, the absorption at longer

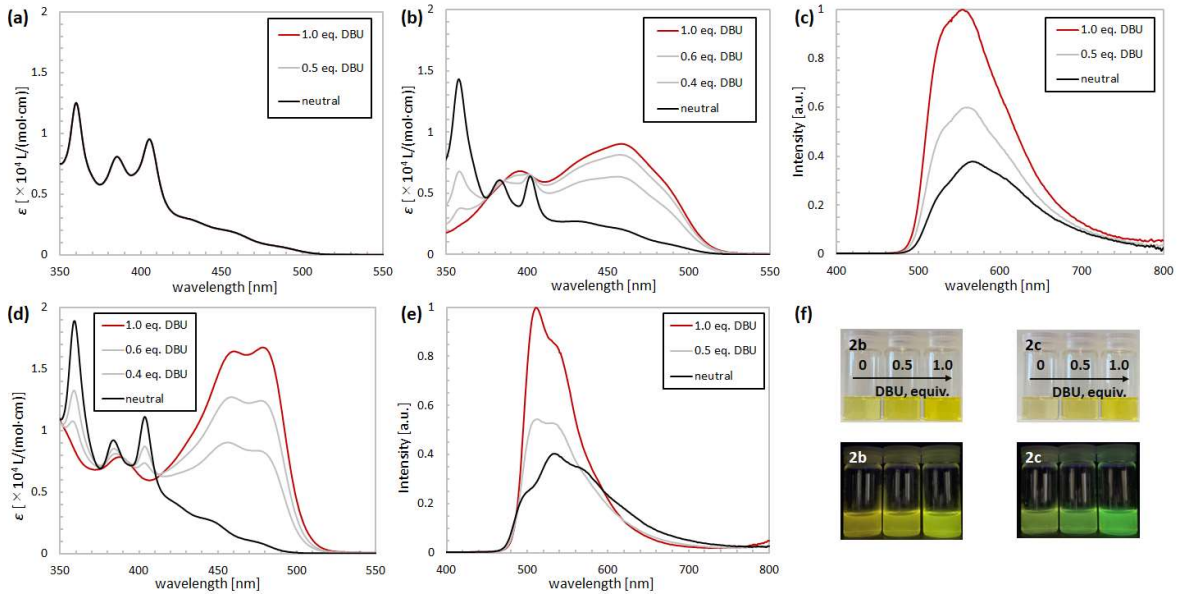

Fig. 4 (a) UV-vis absorption of (a) **4**, (b) **2b**, (d) **2c** and fluorescence spectra of (c) **2b**, (e) **2c** in CH_2Cl_2, added with DBU at 296 K. (f) The colour change of **2b** (left) and **2c** (right) under daylight (above) and 365 nm-UV irradiation (bottom) with addition of DBU.

Table 1 Photophysical properties of the 1-hydroxydibenzofluoranthenes **2** in CH_2Cl_2.[a]

Compounds	Neutral form (no additive)					Anionic form (in the presence of DBU) [b]				
	$\lambda_{Abs.}$ [nm] (ε [10^3 L/(mol cm)])	$\lambda_{Em.}$ [nm]	Φ [%] [c]	τ [ns]	k_F [10^7 s^{-1}] [d]	$\lambda_{Abs.}$ [nm] (ε [10^3 L/(mol cm)])	$\lambda_{Em.}$ [nm]	Φ [%] [c]	τ [ns]	k_F [10^7 s^{-1}] [d]
2a	400 (8.84), 451 (1.92)	543	3.9	3.03	1.29	452 (12.1)	537	8.7	2.80	3.11
2b	402 (6.40), 461 (2.00)	565	3.9	2.85	1.37	458 (9.00)	554	8.9	4.20	2.12
2c	404 (11.1), 450 (2.44)	535	6.3	2.84	1.64	478 (16.7)	511	10	1.60	6.25

a) Both absorption and emission spectra were recorded in solution at room temperature at $c = 5.0 \times 10^{-5}$M. b) Each hydroxydibenzofluoranthene (anionic form) was studied in the presence of DBU (for **2a–c**: 1.0 eq.) c) Quinine sulfate was used as reference dye ($\lambda_{ex} = 366$ nm, $\Phi = 55\%$).[14] d) The radiative rate constants were calculated from the experimentally measured fluorescence quantum yields and lifetimes as $k_F = \Phi/\tau$.

wavelengths red-shifted to 420–630 nm (Fig. 5a, black line), and the bathochromic shift reached saturation with the addition of 30 equivalents of DBU (Fig. 5a, red line). Under basic conditions, the colour of the solution turned red (Fig. 5c, above). The emission spectrum of **3a** showed a peak at 571 nm under neutral conditions (λ_{ex} = 381 nm, Fig. 5b). When 30 equivalents of DBU were added,‡ emission at a longer wavelength of 715 nm was observed, although it was weak (red line). The Φ value of **3a** was very low, 2.7% under neutral conditions and 0.92% under basic conditions. Additionally, the radiative rate constants (k_F) of **3a** decreased with the addition of DBU (1.13×10^7 s^{-1} under neutral conditions, 0.37×10^7 s^{-1} under basic conditions).

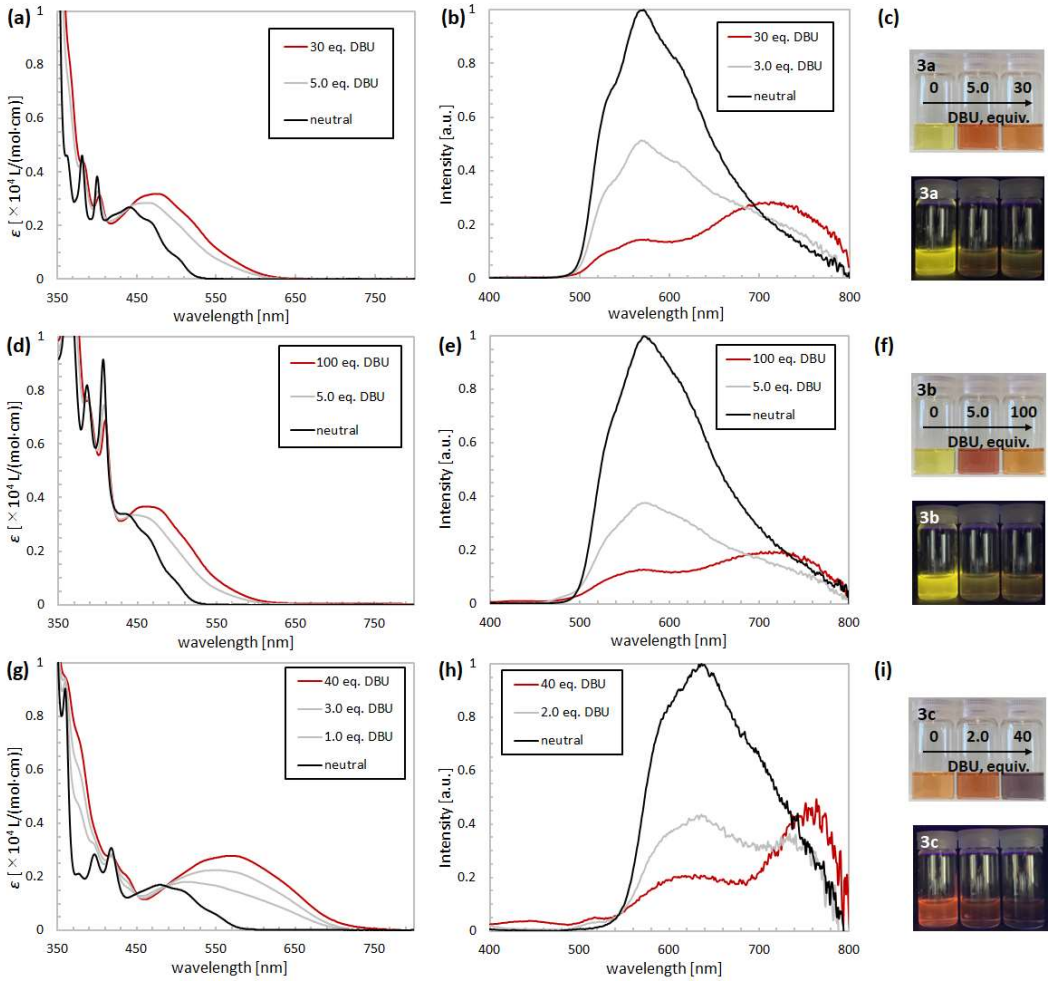

Fig. 5 UV-vis absorption of (a) **3a**, (d) **3b**, (g) **3c** and fluorescence spectra of (b) **3a**, (e) **3b**, (h) **3c** in CH_2Cl_2, added with DBU at 296 K. The colour change of (c) **3a**, (f) **3b** and (i) **3c** under daylight (above) and 365 nm-UV irradiation (bottom) with addition of DBU.

Table 2 Photophysical properties of the hydroxy-dibenzofluoranthenes **3** in CH_2Cl_2.[a]

Compounds	Neutral form (no additive)					Anionic form (in the presence of DBU) [b]				
	$\lambda_{Abs.}$ [nm] (ε [10^3 L/(mol cm)])	$\lambda_{Em.}$ [nm]	Φ [%] [c]	τ [ns]	k_F [10^7 s^{-1}] [d]	$\lambda_{Abs.}$ [nm] (ε [10^3 L/(mol cm)])	$\lambda_{Em.}$ [nm]	Φ [%] [c]	τ [ns]	k_F [10^7 s^{-1}] [d]
3a	400 (3.84), 442 (2.68)	571	2.7	2.40	1.13	475 (3.18)	715	0.92	2.50	0.37
3b	407 (9.16), 440 (3.34)	572	2.8	2.11	1.33	462 (3.66)	725	1.5	2.37	0.63
3c	418 (3.08), 480 (1.70)	640	0.57	—	—	570 (2.78)	764	0.30	—	—

a) Both absorption and emission spectra were recorded in solution at room temperature at $c = 5.0 \times 10^{-5}$ M. b) Each hydroxy-dibenzofluoranthene (anionic form) was studied in the presence of DBU (for **3a**: 30 eq.; **3b**: 100 eq.; **3c:** 40 eq.) c) Quinine sulfate was used as reference dye ($\lambda_{ex} = 366$ nm, $\Phi = 55\%$).[14] d) The radiative rate constants were calculated from the experimentally measured fluorescence quantum yields and lifetimes as $k_F = \Phi/\tau$.

The absorption and fluorescence spectra of **3b** were similar to those of **3a**, indicating that the introduction of an electron-donating group at the 1 position barely affected the photophysical property of **3** (Fig. 5d–f). In contrast, substitution with an electron-withdrawing group at the 1 position (**3c**) resulted in absorption at longer wavelengths than both **3a** and **3b** under neutral conditions (Fig. 5g). A bathochromic shift was observed for **3a-c** upon the addition of DBU. Notably, 1-cyano-9-hydroxy **3c** exhibited a red-shifted absorption of more than 100 nm and near-infrared (NIR) fluorescence (λ_{em} = 764 nm, λ_{ex} =365 nm) under basic conditions (Fig. 5h). When comparing the donor-π-acceptor type molecules **2c** and **3c**, the introduction of the CN group at the 9 position in 1-hydroxydibenzofluoranthene (**2c**) had little effect on the absorption and fluorescence. However, the introduction of this electron-withdrawing group at the 1 position of the 9-hydroxy group (**3c**) resulted in a significant bathochromic shift.

2.3 Solvatochromic properties of 2c and 3c

The effect of the solvent on the chromic property was also examined. The UV-vis and fluorescent spectra of **2c** and **3c** in DMSO, an aprotic polar solvent, are shown in Fig. 6. Similar to observation in CH_2Cl_2, a hyperchromic shift of **2c** was noted in DMSO under basic conditions. However, unlike in CH_2Cl_2, the addition of TFA reduced the longer wavelength absorption of **2c**. These results indicate that DMSO may partially deprotonate the phenolic proton of **2c**, even under neutral conditions. When comparing the absorption wavelength (λ_{Abs}) in DMSO with those in CH_2Cl_2, it was found that **2c** exhibited a longer λ_{Abs} under both neutral and basic conditions.

In contrast, under neutral conditions the UV-vis absorption of **3c** in DMSO was similar to that in CH_2Cl_2, but λ_{Abs} was red-shifted by 110 nm under basic conditions. Surprisingly, **3c** in DMSO exhibited an absorbance wavelength of 680 nm under basic conditions, reaching the NIR region.

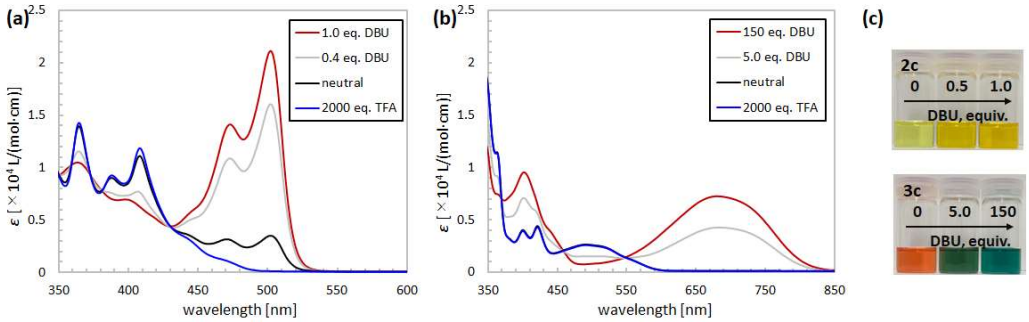

Fig. 6 UV-vis absorption of (a) **2c** and (b) **3c** in DMSO, added with DBU or TFA at 296 K. (c) The colour change of **2c** (above) and **3c** (bottom) under daylight (above) in neutral or basic conditions.

2.4 Calculation Study

To gain insight into the photophysical properties of hydroxydibenzofluoranthenes, time-dependent density functional theory (TD-DFT) calculation using B3LYP/6-31+G(d,p) basis set with solvation model in CH_2Cl_2 was performed. A comparison of the crystal structure of compound **2b** with all bond distances obtained from the calculations confirms their validity (see SI; Fig. S2). The frontier molecular energy levels, electron density distributions of the highest occupied molecular orbital (HOMO) and lowest unoccupied molecular orbital (LUMO), and oscillator strength (*f*) for **2a**, **2c**, **3a**, and **3c**, along with their corresponding anions, were summarized in Fig. 7a (for **2b** and **3b**, see SI; Fig. S10). In the neutral forms of compounds **2** and **3**, the electron density in the HOMO orbitals is localized along the long axis of the phenanthrene (**ABC**) and naphthalene (**EF**) rings. Conversely, their LUMO orbitals are aligned parallel to the short axis of these rings, with a large density is localized concentrated on the central pentagon (**D**). Deprotonation of both hydroxydibenzofruorathenes **2** and **3** significantly alters the electron density distribution in the

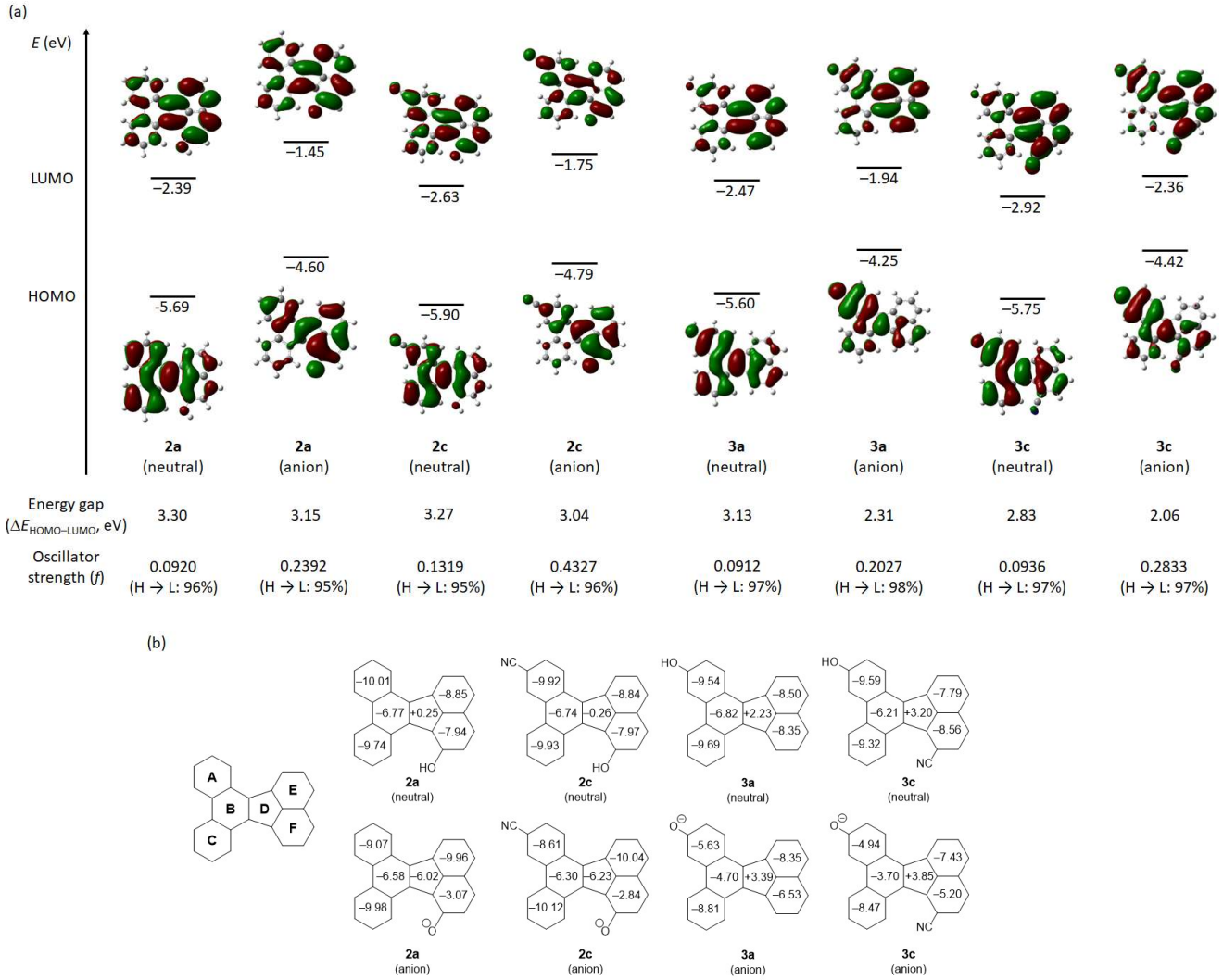

Fig. 7 (a) Calculated frontier molecular orbitals, energy levels ($\Delta E_{HOMO-LUMO}$) and oscillator strengths (*f*) of **2a**(neutral, anion), **2c**(neutral, anion), **3a**(neutral, anion) and **3c**(neutral, anion) at the B3LYP/6-31+G(d,p)-CPCM(DCM). The contribution of the HOMO to LUMO transition is shown in parentheses below the f value. (b) NICS(1) values of **2a**(neutral, anion), **2c**(neutral, anion), **3a**(neutral, anion) and **3c**(neutral, anion) at the GIAO/B3LYP/6-31+G(d,p).

HOMO orbital. For the anionic forms of **2** and **3**, the electron density of the HOMO orbital delocalizes across the **ABDEF** rings, indicating cross-conjugation of the phenanthrene and naphthalene rings under basic conditions. However, the density of LUMO orbital of **2**(anion) and **3**(anion) remains quite similar to that of **2**(neutral) and **3**(neutral), respectively. The HOMO-LUMO energy gap ($\Delta E_{HOMO-LUMO}$, eV) and the oscillator strength (*f*) are in good agreement with observed trends in UV-vis absorption. For the series of 1-hydroxyfluoranthenes **2** exhibiting a hyperchromic shift, the respective $\Delta E_{HOMO-LUMO}$ values for the neutral and anionic species are comparable [**2a**(neutral); 3.30 eV vs **2a**(anion) 3.15 eV, **2c**(neutral); 3.27 eV vs **2c**(anion) 3.04 eV], and the *f* values of the anionic species are significantly higher than those of the neutral species [**2a** (neutral); 0.092 vs **2a** (anion) 0.239, **2c** (neutral); 0.132 vs **2c** (anion) 0.433]. These calculations also explain the observed bathochromic shift of 9-hydroxyfluoranthenes **3**. $\Delta E_{HOMO-LUMO}$ and *f* values significantly decreased and increased, respectively, upon transformation of **3**(neutral) into **3**(anion). Those changes suggest that the absorption of **3**(anion) would be observed at longer wavelength and stronger than that of **3**(neutral).

Nucleus-independent chemical shifts (NICS) were calculated to estimate the local aromaticity of each ring in both the neutral and anionic forms of **2** and **3** (Fig. 7b; for **2b** and **3b**, see SI; Tables S19,20, 25 and 26). For the neutral forms of **2** and **3**, the NICS(1) values for rings **A**, **B**, **C**, **E** and **F** ranged between –7.79 and –10.0, while the NICS(1) value for ring **D** varied from +3.20 to –0.20. These results indicate that, under neutral conditions, the phenanthrene (**ABC**) and naphthalene (**EF**) rings exhibit almost independent aromatic characteristics, and the central pentagon is non-aromatic or weak anti-aromatic. The HOMA values for compound **2b**, whose X-ray crystal structure was obtained, are consistent with the aromaticity predictions derived from the NICS(1) values (see SI; Table S3). For the

anionic species of **2**, the NICS(1) value of ring **F** increases significantly, whereas that of ring **D** decreases compared to their neutral counterparts. This suggests that the anion form of **2** makes a fluorenyl-anion-type resonance structure, as illustrated in Fig. 1, with large contribution. In contrast, for **3**(anion), the NICS(1) values of rings **A**, **B** and **F** are considerably higher than those of **3**(neutral), indicating a weakening in the aromatic character of those rings in the anion form of **3**. Additionally, the local anti-aromatic character of ring **D** slightly intensifies under basic conditions, implying that an increased contribution of quinoid resonance. These calculation studies effectively elucidate that the distinctive chromic properties of **2** and **3** result from different resonance hybrids.

3. Conclusion

In this study, we synthesised new halochromic fluoranthene derivatives and found that even though the same chromophore skeleton was employed, altering the positions of the auxochromes resulted in contrasting halochromic properties under basic conditions. Notably, 9-hydroxydibenzofluoranthenes **3** exhibit emissions red-shifted by almost 200 nm compared to 1-hydroxy compounds **2**. TD-DFT and NICS calculations supported the idea that the characteristic chromic properties of fluoranthenes are based on changes in the resonance structures of the cross-conjugated system.

Conflicts of interest

There are no conflicts to declare.

Acknowledgements

This work was supported by JSPS KAKENHI (Grant Numbers 23K18183 and 23K27295) and MEXT KAKNHI (Grant Number JP21H05211) in Digi-TOS and BINDS from AMED (Grant Numbers 22ama121042j0001 and 22ama121034j0001). K.K. acknowledges support from Sasakawa Scientific Research Grant and JST SPRING (JPMJSP2110).

References

‡ The amount of base required for complete deprotonation depends on the pK_a value of **2a** (12.9±0.2 in DMSO) and **3a** (14.2 ±0.3 in DMSO).

1 H. Almasi, S. Forghani and M. Moradi, *Food Packag. Shelf Life*, 2022, **32**, 100839.
2 (*a*) P. R. Somani and S. Radhakrishman, *Mater. Chem. Phys.*, 2002, ***77***, 117. (*b*) Y. Ke, C. Zhou, Y. Zhou, S. Wang, S. H. Chan and Y. Long, *Adv. Funct. Mater.*, 2018, **28**, 1800113.
3 (*a*) A. Steinegger, O. S. Wolfbeis and S. M. Borisov, *Chem. Rev.,* 2020, **120**, 12357; (*b*) N. Bar and P. Chowdhury, *ACS Appl. Electron. Mater*., 2022, **4**, 3749.
4 (*a*) K. Taguchi, *J. Am. Chem. Soc.*, 1986, **108**, 2705. (*b*) A. Singh, R. Choi, B. Choi and J. Koh, *Dyes Pigm.*, 2012, **95**, 580.
5 (*a*) Y. Dong, J. W. Y. Lam, A. Qin, Z. Li, J. Liu, J. Sun, Y. Dong and B. Z. Tang, *Chem. Phys. Lett.*, 2007, **446**, 124. (*b*) H. long, D. Guo, L. Wang, Z. Liu, S. Li, X. Liang, Y. Chen, Z. Yang, J. Li, L. Dong and L. Tan, *Dyes Pigm.*, 2022, **203**, 110330.
6 (*a*) G. Laus, H. Schottenberger, K. Wurst, J. Schütz, K. H. Ongania, U. E. I. Horvath and A. Schwärzler, *Org. Biomol. Chem.,* 2003, **1**, 1409; (*b*) H. Enozawa, S. Ukai, H. Ito, T. Murata and Y. Morita, *Org. Lett.,* 2019, **21**, 2161; (*c*) W. Chen, S. Liu, Y. Ren, S. Xie, C. Yan, Z. Zhou and G. Zhou, *Chem. Eur. J.*, 2023, **29**, e202203238.
7 A. Wetzel, T. Alexander, S. Brandt, R. Haas and D.Werner, *Bull. Environ. Contam. Toxicol.,* 1994, **53**, 856.
8 (*a*) G. Brauers, R. Ebel, R. Edrada, V. Wray, A. Berg, U. Gräfe and P. Proksch, *J. Nat. Prod.,* 2001, **64**, 651; (*b*) K. Koyama, D. Kuramochi, K. Kinoshita, and K. Takahashi, *J. Nat. Prod.,* 2002, **65**, 1489; (*c*) L. Du, J. B. King and R. H. Cichewicz, *J. Nat. Prod.,* 2014, **77**, 2454.
9 (*a*) N. Venkatramaiah, S. Kumar and S. Patil, *Chem. Commun.*, 2012, **48**, 5007; (*b*) A. Goel, A. Sharma, M. Kathuria, A. Bhattacharjee, A. Verma, P. R. Mishra, A. Nazir and K. Mitra, *Org. Lett.,* 2014, **16**, 756; (*c*) I. Kawajiri, M. Nagahara, H. Ishikawa, Y. Yamamoto, J. Nishida, C. Kitamura and T. Kawase, *Can. J. Chem.,* 2017, **95**, 371; (*d*) J. Yang, M. Horst, S. H. Werby, L. CegeIski, N. Z. Burns and X. Yang, *J. Am. Chem. Soc.,* 2020, **142**, 14619; (*e*) W. Shi, X. Yang, X. Li, L. Men, D. Zhang, Z. Zhu, X. Xiao and D. Zhao, *Chem. Eur. J.,* 2022, **28**, e202104598.
10 H. Wu, R. Fang, J. Tao, D. Wang, X. Qiao, X. Yang, F. Hartl and H. Li, *Chem. Commun.,* 2017, **53**, 751.
11 W. Wu, J. Li, F. Guo, L. Zhang, Y. Long and J. Hua, *Renew. Energ.,* 2010, **35**, 1724.
12 (*a*) C. F. H. Allen and J. A. VanAllan, *J. Org. Chem.,* 1952, **17**, 845; (*b*) M. Yamaguchi, M. Higuchi, K. Tazawa and K. Manabe, *J. Org. Chem.,* 2016, **81**, 3967; (*c*) J. Karunakaran and A. K. Mohanakrishnan, *Eur. J. Org. Chem.,* 2017, 6747; (*d*) S. Pal, Ö. Metin and Y. E. Türkmen, *ACS Omega,* 2017, **2**, 8689; (*e*) H. Takano, N. Shiozawa, Y. Imai, K. S. Kanyiva and T. Shibata, *J. Am. Chem. Soc.,* 2020, **142**, 4714; (*f*) S. Yang and Y. Zhang, *Org. Lett.,* 2022, **24**. 9060.
13 N. Ogawa, Y. Yamaoka, K. Yamada, K. and K. Takasu, *Org. Lett.,* 2017, **19**, 3327.
14 C. A. Parker and W. Rees, *Analyst,* 1960, **85**, 587.